

Article

Chlorine vs. Sodium Chloride Regeneration of Zeolite Column for Ammonium Removal from an Explosives Impacted Mining Wastewater

Tianguang Zhang ¹ , Roberto M. Narbaitz ^{1,*}, Majid Sartaj ¹ and Jason Downey ²¹ Department of Civil Engineering, University of Ottawa, 161 Louis Pasteur Pvt., Ottawa, ON K1N-6N5, Canada² Dowclear Inc., 627 South Island Park Drive, Manotick, ON K4M-1J2, Canada

* Correspondence: narbaitz@uottawa.ca

Abstract: There has only been limited research on ammonium removal by zeolites followed by chlorine regeneration; these studies used batch tests and, in many cases, only dealt with single solute solutions as opposed to multi-component ones. To better simulate full-scale applications, this study used a continuous-flow ion exchange (IE) column system to assess the feasibility of chlorine regeneration of a zeolite IE column used for the removal of ammonium from synthetic explosives impacted mining wastewater (EIMWW). Multi-cycle column loading-regeneration tests were used to evaluate and compare the performance of a NaOCl (1000 ppm as free Cl₂) solution with that of a standard salt regeneration solution (5% NaCl). In addition, the impact of two loading cycle durations was evaluated. After three operational cycles with 6 h loading phases, the TAN (total ammonia nitrogen) uptake after NaOCl regeneration was almost the same as that obtained with salt regeneration (0.21 meq/g vs. 0.21 meq/g). The zeolite with NaOCl regeneration showed a higher preference for TAN than with NaCl regeneration (Ca:TAN:K = 2.8:2.3:1 vs. 2.5:1.9:1 for the 6 h loading phase); however, the NaOCl regeneration took longer to complete. It was also found that effluent pH, total chlorine level, and free chlorine level during the chlorine regeneration were positively related, seemingly confirming that the ammonium is oxidized to nitrogen gas and producing hydrogen ions. Regardless of the regeneration solution, if one uses a two-column system, with one column online and the other offline, the shorter loading cycles (6 h) yield a substantially higher daily TAN removal rate.

Keywords: ion exchange column; zeolite; ammonium removal; chlorine regeneration; sodium chloride regeneration



Citation: Zhang, T.; Narbaitz, R.M.; Sartaj, M.; Downey, J. Chlorine vs. Sodium Chloride Regeneration of Zeolite Column for Ammonium Removal from an Explosives Impacted Mining Wastewater. *Water* **2022**, *14*, 3094. <https://doi.org/10.3390/w14193094>

Academic Editor: Wei Wei

Received: 1 September 2022

Accepted: 29 September 2022

Published: 1 October 2022

Publisher's Note: MDPI stays neutral with regard to jurisdictional claims in published maps and institutional affiliations.



Copyright: © 2022 by the authors. Licensee MDPI, Basel, Switzerland. This article is an open access article distributed under the terms and conditions of the Creative Commons Attribution (CC BY) license (<https://creativecommons.org/licenses/by/4.0/>).

1. Introduction

Due to the extensive use of ammonium nitrate explosives in the mining industry, mining wastewaters are a significant source of ammonia pollution in aquatic environments [1,2]. Pommen [3] reported that explosive impacted mining wastewater (EIMWW) had total ammonia nitrogen (TAN) concentrations in the 0.3 to 80 mg as N/L range. NH₃ is highly toxic to aquatic organisms [4–6]. The threshold acute lethal level (i.e., 50% rainbow trout lethality in 96 h) for wastewater effluents was reached when ammonia concentrations were as low as 2 mg TAN as N/L [7,8].

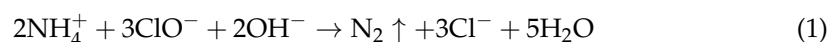
Canadian mines are subject to very low temperatures, so ion exchange (IE) is an appropriate technology for these applications while biological ammonium removal is not as suitable due its temperature sensitivity. In addition, most mining projects are located in very isolated and remote areas with poor accessibility and a lack of skilled personnel to support large-scale treatment plants. Thus, IE is particularly suitable for mining applications based on its rapid start-up and full automation.

Cationic ion exchangers are able to adsorb ammonium (NH₄⁺) which is the major form of ammonia at neutral pH levels. Zeolite, as a cationic ion exchanger, has been widely researched for TAN removal because of its good TAN removal capacity, low price, and high availability in nature [9,10]. However, many of these studies used single-solute ammonium

solutions, while practical applications involve wastewaters with many ions that compete for IE sites. Clinoptilolite, a common type of zeolite, was studied by Ames [11] who found through multiple column tests that ammonium is somewhat preferred over some major exchanged cations including some divalent ions, such as calcium [9,12]. In this preference sequence, potassium outcompetes ammonium [11,13,14]. Hence, clinoptilolite will be less effective for ammonium removal from wastewaters due to the presence of these competing ions, particularly because of competition with potassium [2].

To restore the uptake capacity of the ion exchanger they should be regenerated frequently; the standard regenerants for zeolites are 0.5 to 10% NaCl solutions [15–19]. The used regeneration solution contains high concentrations of TAN and NaCl so it cannot be released into the environment without treatment. In addition, it is not practical to recycle the regeneration solution for the next regeneration cycle without eliminating a significant portion of the TAN from it. Therefore, the treatment of used salt regeneration solutions becomes an environmental and operational challenge. A number of studies have used air stripping to remove ammonia from the used regeneration solution [15,20–22], however, this is not an effective technology in frigid climates such as in Canada. Thus, a different regeneration method is needed.

Using hypochlorite solutions to regenerate the ammonium-loaded zeolite is one such approach. Huang et al. [23] and Zhang et al. [24] claimed that the ammonia nitrogen could be released from ion exchange material and converted to N₂ gas through chlorination, thus the ammonia is removed from the regeneration solution and prevents the above-mentioned secondary pollution. They suggested it occurred by the following chemical reaction:



Zhang et al. [24] only studied the regeneration of a zeolite loaded with a single-solute ammonium solution. Huang et al. [23] used multi-ion synthetic swine wastewater; however, they did not thoroughly study the removal of the other ions. A potential difficulty of the chlorine regeneration method is that the regeneration of IE sites is likely going to be limited [25]. This may reduce the number of sites available for TAN, resulting in a reduction in the subsequent TAN uptakes. In addition, the standard ion exchange systems consist of continuous flow column systems, while both Huang et al. [23] and Zhang et al. [24] only evaluated the regeneration efficiency of batch mode systems. Due to competitive ion uptake effects, limited flow contact time with the media, and possibly different ion diffusion rates, the ion preference for column systems may be different from that for batch (equilibrium) systems [2].

In this study, the feasibility of using a NaOCl solution to regenerate a zeolite was assessed for more realistic conditions, that is by conducting multiple loading and regeneration cycles using a continuous flow column to treat a multi-ion (TAN, calcium, and potassium) synthetic EIMWW. For comparison, experiments were also performed using a standard NaCl regeneration solution.

2. Experimental Materials and Methods

2.1. Materials

A commercial natural zeolite (SIR-600, ResinTech Inc., Camden, NJ, USA) was used for this study because it performed well for TAN uptake in an earlier study [2]. Although the supplier does not disclose its mineralogy or source, Chartrand [18] found it to perform similarly to a clinoptilolite from another supplier. Particle size distribution analysis of the media by via sieve analysis was performed using ASTM D6913/D6913M-17 [26]. It showed that 89% of the media particles were in the 0.59 to 1.68 mm range, an additional 5% of the media was in the 0.4 to 0.59 mm range, and the rest consists of smaller particles [25]. A N₂ adsorption-based surface area analyzer (ASAP 2020, Micromeritics, Norcross, GA, USA) was used to determine the BET surface area of SIR-600, it was 16 m²/g [25].

The loading experiments were conducted using synthetic EIMWW wastewater because an actual EIMWW was not available. It was prepared with ammonium chloride, potassium

chloride and calcium chloride hexahydrate (ACS grade, Fisher Scientific, Waltham, MA, USA). The synthetic wastewater had approximately 21 mg TAN as N/L, 30 mg K/L, and 80 mg Ca/L (1.5 meq/L, 0.77 meq/L, and 4 meq/L, respectively). These concentrations are close to those reported for underground mining wastewater [19] (20 mg TAN as N/L, 14 mg K/L, and 87 mg Ca/L).

Two main regenerant solutions were used in this study, a NaOCl solution and a NaCl solution. The NaOCl regeneration solution was obtained by the dilution of commercial bleach. The 1000 mg free Cl₂/L solution was chosen because it provided a sufficient quantity of chlorine required to oxidize the TAN loaded on the zeolite during the experiments (i.e., Cl₂:N mass ratio > 8). The 5% NaCl regenerant was prepared by dissolving solid NaCl (ACS grade, Fisher Scientific, Waltham, MA) in distilled water. The 5% NaCl solution was selected because a previous study indicated this concentration was nearly as effective for SIR-600 regeneration as 10% NaCl [16]. The pH of the NaCl regeneration solutions was adjusted to pH = 10, to enhance the regeneration based on the shift from NH₄⁺ to NH₃ at this pH. The column experiments were primarily intended to compare the multiple-cycle performance of the two regenerants. The ion uptake of zeolite in the subsequent cycle was calculated to evaluate and compare the effectiveness of the two regenerant solutions.

2.2. Analytical Methods

Total ammonia nitrogen (TAN) concentration was quantified using a modified version of the Nessler method from Standard Method 4500-NH₃ C [27]. The resulting colour was quantified in terms of the absorbance at a wavelength of 425 nm using a spectrophotometer (DR6000, Hach, Loveland, CO, USA). The Ca and K ion concentrations were quantified using a procedure adapted from Standard Method 3111B [28] using a flame atomic absorption spectrometer (AAS) (PinAAcle 500, PerkinElmer, Waltham, MA, USA). Free and total chlorine concentrations were measured using Hach method 8021 and 8167 (equivalent to Standard Method 4500-Cl G for drinking water) [28]. pH values were analyzed with a pH meter (VER Symphony B10P, VWR, Radnor, PA, USA) with a pH probe (VWR 89231-580, VWR, Radnor, PA, USA).

2.3. Experimental Methods

2.3.1. Column Setup

Bench-scale continuous flow column studies were conducted to assess SIR-600's performance in the removal of TAN from EIMWW. A clear glass column with 2.2 cm inner diameter (ID) and 110 cm length (Ace Glass, Vineland, NJ, USA) was used for these tests. 96.1 g SIR-600 (dry weight) were loaded into the column which resulted in an IE bed depth of 30.5 cm and a bed volume (BV) of 116 cm³. A coarse sintered glass disc in the column supported the IE materials. A stopcock at the bottom of the column was used to stop the flow from the column when needed. The flowrate of the loading solution was maintained at approximately 50 mL/min (25.9 BVs/h) by a high-pressure liquid metering pump (Optos Model3, Eldex, Napa, CA, USA). The effluent flowrate was occasionally monitored by weighing the mass of effluent collected over one minute, and the pump setting was adjusted if it was necessary. The column delivered the EIMWW to the top of the column from where it flowed through the SIR-600 bed in the down-flow direction. The performance of the IE system was evaluated using multiple cycles to approximate the long-term performance of the system. Each cycle of a column test was divided into two parts: a loading phase and a regeneration phase.

In all the loading phases the same synthetic EIMWW was used as the influent; the effluent TAN, Ca and K concentrations were monitored at regular intervals. The ion uptake of the SIR-600 column in the loading phase can be calculated using an integral mass balance of the ion, the resulting equation is:

$$q = \frac{\int_{V=0}^{V=\text{loading phase end}} (C_{\text{inf}} - C_{\text{eff}}) dV}{M} \quad (2)$$

where q is the ion uptake of the SIR-600 (meq/g), V is the volume of liquid treated (L), which changes with time; C_{inf} is the influent ion concentration (meq/L); C_{eff} is the effluent ion concentration (meq/L), which changes with V and time; and M is the mass of SIR-600 (g) in the column. The integration was performed using the trapezoidal rule.

During the regeneration phases the regeneration solution was also circulated in the down-flow mode. The regenerant flowrate was delivered using a peristaltic pump (Masterflex L/S variable-speed economy drive, Cole-Parmer, Vernon Hills, IL, USA).

Four sets of tests were performed to study the feasibility of the loading-regeneration cycles with different durations. Two of the sets used a 5% NaCl regeneration solution and two used a 1000 mg free Cl_2 /L regeneration solution. For each regenerant, the first set of tests had 23 h long loading phases and were intended to saturate or nearly saturate the IE media. Furthermore, the second sets had 6 h long loading phases and were intended to simulate more realistic operating conditions. The cycles were named using the following XY# system. Where X equals S or C representing salt or chlorine, respectively; Y equals L or S representing the 23 h and 6 h loading cycles, respectively; and # denotes the number of the cycle. For example, SS#3 denotes the third 6 h loading run preceded by salt regeneration and CL#2 denotes the second 23 h loading run preceded by chlorine regeneration.

2.3.2. Chlorine Regeneration

As mentioned earlier, hypochlorite regeneration in a continuous-flow column system is part of the novelty of this study. The first chlorine regeneration cycle (CL1) was initiated with a 50 mL/min (25.9 BVs/h) regeneration flowrate. However, this led to the formation of many bubbles within the column, which constrained the flow and made the flowrate unstable. Accordingly, the average regenerant flowrate was reduced to 20 mL/min (10.3 BVs/h); it was monitored regularly and adjusted if necessary. As the regeneration kinetics were not known, the chlorine regeneration duration for the 23 h loading phase was chosen to be 3.4 h, which is comparable to that used for the salt regenerations. Since these cycles were not so effective, the CS cycles used proportionally longer regeneration period (4 h). In addition, the regenerant flowrate for the CS runs was reduced to 16 mL/min to provide greater stability. Before each series of column tests (i.e., CL and CS), the zeolite was preconditioned with 5% NaCl solution to ensure the loading performances in the first loading phases of the chlorine cycles was equivalent to those of the first salt regeneration cycles. The operating cycles with different durations and regenerant type are summarized in Table 1.

Table 1. Operating cycles characteristics and codes.

Regenerant Type	Loading Cycle/Regeneration Cycle Duration	Cycle Codes
NaOCl	23 h/6 h	CL1
		CL2
	6 h/3.4 h	CS1 CS2 CS3
NaCl	23 h/3 h	SL1 SL2
		6 h/1 h

2.3.3. NaCl Regeneration

After both the SL and SS loading cycles, the regenerant flowrate was 16 mL/min (8.3 BVs/h). For the SL cycle tests, the 23 h loading phases plus a three-hour regeneration phase was performed between two loading phases, so each regeneration used 25 BVs of

regenerant. For the SS, the three 6 h loading phases were followed by 1 h regeneration phases, so they used 8.3 BVs of regenerant per cycle.

3. Results and Discussions

3.1. Cycles for the 23 h Loading Phases with Chlorine Regeneration

To test the feasibility of chlorine regeneration to restore the TAN uptake capacity of a SIR-600 packed column, two cycles with 23 h column loading phases were performed (CL1 & CL2). Accordingly, only CL2 is representative of the impact of chlorine regeneration and is the focus of the discussion. The second CL cycle's breakthroughs occurred a bit earlier than the first cycle's as the column was adjusting to the change in regenerant solution and regeneration cycle length. The following observations can be made from the ion breakthrough curves for the CL2 cycle (Figure 1a). First, the normalized effluent ion concentrations (i.e., $C_{\text{eff}}/C_{\text{inf}}$) reach a value of 1, so the column becomes saturated for the three ions after approximately 380 BVs (~900 min). Thus, using chlorine regeneration the loading runs should be less than 960 min. Second, the order of the ion breakthroughs is Ca then K and finally TAN, however K and TAN saturate at approximately the same time. Third, after 150 bed volumes of water are treated, the normalized effluent Ca concentration (i.e., $C_{\text{eff}}/C_{\text{inf}}$) slightly exceeds 1, indicating that some previously sorbed Ca is being displaced. This is presumably due to the competition with TAN and K.

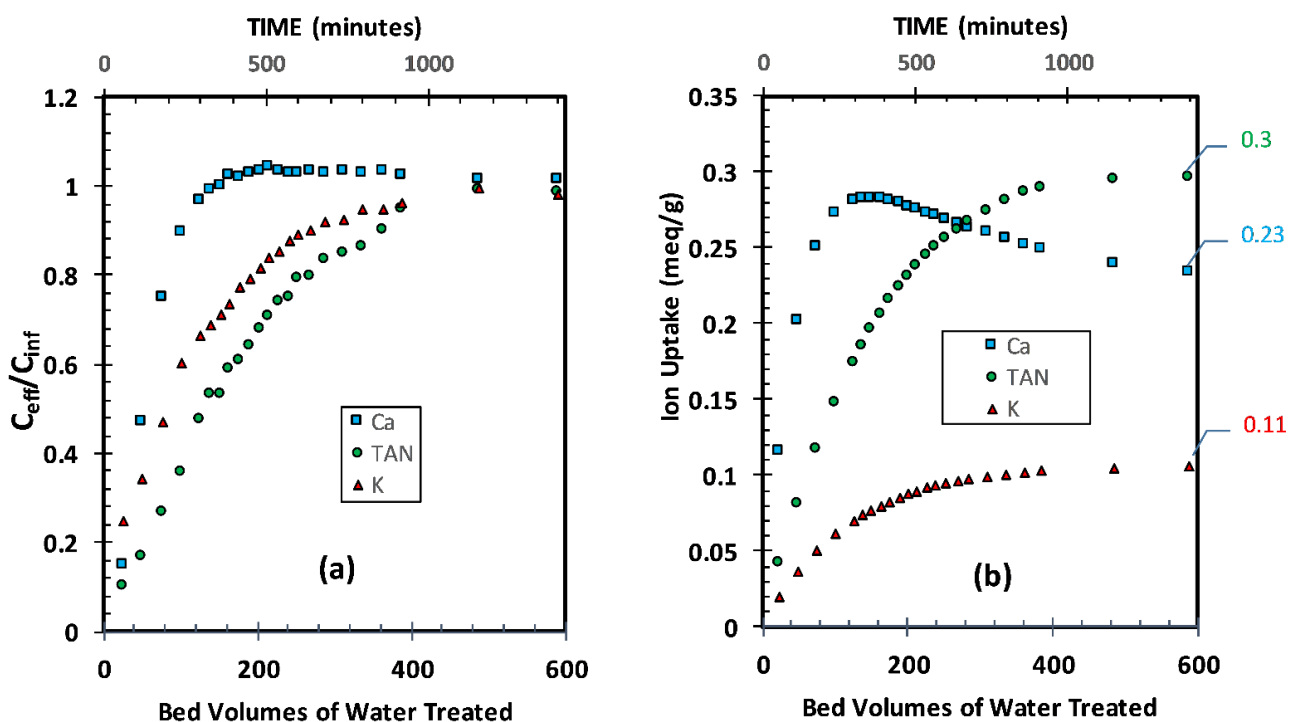
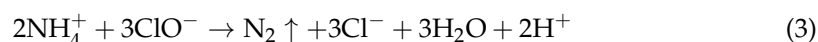


Figure 1. Second 23 h loading cycle with chlorine regeneration (CL2): (a) breakthrough; (b) ion uptake versus bed volumes of water treated.

The breakthrough results yielded the cumulative uptake curves shown in Figure 1b, its key features are as follows. First, the three ions appear to reach saturation levels as the uptakes appear to reach plateau values. Second, the Ca uptake peaks at around 150 bed volumes of water treated and then decreases as expected from the $C_{\text{eff}}/C_{\text{inf}}$ values greater than 1 in Figure 1a. Thus, the Ca appears to be displaced due to competition with the TAN and K. Third, by the end of the loading phase the column achieves a saturation TAN uptake of 0.3 meq TAN/g. There are no previous studies with chlorine regeneration; however, this value is within the 0.073 to 0.5 meq/g range reported in the literature for NaCl regeneration [15,20,21]. Fourth, the column achieves significantly higher TAN:K uptake ratios (2.7 to 1) than observed by Ames [11]. He observed a general selectivity order

of $K > TAN$ in his experiments using solutions with equal ion concentrations, in the current study's EIMWW the TAN/K ratio was 1.95. In addition, the higher TAN than K uptake is consistent with the findings of Chartrand et al. [2] using the same media. On the other hand, the TAN:K uptake ratio in CL2 is significantly higher than that in CL1 (1.3 to 1, data not shown). The probable reason for the relatively higher TAN uptake is that chlorine regeneration primarily targets SIR-600 sites occupied by ammonium during regeneration, because of the reaction between the OCl^- in the regenerant and the ammonium in the column during the regeneration phase.

The reaction stoichiometry suggested by Zhang et al. [24] was presented as Equation (1). That equation is equivalent to the overall reaction of breakpoint chlorination [29]:



Thus, during the NaOCl regeneration, the ammonium was oxidized into nitrogen gas which left the system. The bubbles generated in the column during the regeneration of the SIR-600 bed suggest that this reaction was taking place. Because of the reaction, the regeneration of the Ca and K occupied sites likely occurred by IE, with the limited quantities of Na introduced through the NaOCl solution. The hypochlorite solution introduces approximately 324 mg Na/L (assuming NaOCl is the only Na source in the original bleach) while the 5% NaCl regeneration solution contains 19,658 mg Na/L. Thus, the Ca and K uptakes are lower than the TAN uptakes in the CL2 loading phase. Note that if Ca and K uptake after the NaOCl regeneration were to only take place on sites previously occupied by TAN, then this uptake would be limited to the decrease of the TAN uptake between the first and second loading cycle. Since this difference is only 0.09 meq/g (i.e., $0.39 - 0.3$ meq TAN/g) while $q_{Ca} + q_K$ in the second loading cycle is 0.34 meq/g suggests that the sodium in the NaOCl solution played a role in the column regeneration.

3.2. Cycles for the 6 h Loading Phases with Chlorine Regeneration

To further compare NaOCl regeneration with NaCl regeneration, a set of column runs with 6 h loading cycles were performed, these are referred to as the CS cycles. The breakthroughs in the loading phases of the CS cycles shifted to the left as the column equilibrated to the regeneration solution (as the first loading was conducted with media conditioned with 5% NaCl solution) and the different cycle lengths. The second and third cycles yielded similar breakthroughs, thus the analysis will continue based on the third cycle which should be the most representative of the new set of operating conditions. As expected, the ion breakthroughs (Figure 2a) followed the same order as in the CL2 (Figure 1a) and only the Ca concentration of effluent approached that of feed solution by the end of the CS3 loading phase. The K and TAN concentrations in the effluent reached approximately 54% and 43% of the influent concentrations by the end of the CS3 loading phase. This breakthrough data was used to construct a graph of the loading phase's cumulative ion uptakes versus bed volumes of water treated (Figure 2b). First, uptakes follow a similar pattern and similar values to those in the 23 h loading phase. For example, the column becomes saturated with Ca after about 100 bed volumes of water is treated, as in the 23 h loading phase. Second, at the end of the 6 h loading phase Ca has the highest uptake as opposed to the TAN uptake at the end of the 23 h loading phase. However, after 150 BVs of water treated, the ion uptakes are similar (Ca:TAN:K = 0.26:0.21:0.09 for CS3 vs. 0.28:0.2:0.08 for CL2 (Figure 1b)). Third, the TAN uptake is significantly higher than that of K (0.21 vs. 0.09 meq/g at the end of the CS3 loading phase). Fourth, the rate of TAN uptake increases slightly faster than that of K, the TAN:K ratio increased slightly from 2.1:1 at 25 BV to 2.3:1 at 144 BV. The TAN:Ca cumulative uptake ratio also increased with bed volumes of treated water (e.g., 0.42:1 at 25 BVs to 0.83:1 at 144 BVs). Thus, the relative TAN uptake in CS3 increased slightly with an increasing number of bed volumes treated. Finally, if the NaOCl solution only regenerated the sites containing TAN, then the total ion uptake ($q_{Ca} + q_{TAN} + q_K$) in the last loading cycle should be less than or equal to the TAN uptake in the previous loading cycle. As shown by Figure 3, for CS3, $q_{Ca} + q_{TAN} + q_K$ is

approximately 0.56 meq/g which is much larger than the 0.21 meq/g TAN uptake of the second cycle (CS2). This indicates that the Na in the NaOCl has a significant role in the column regeneration.

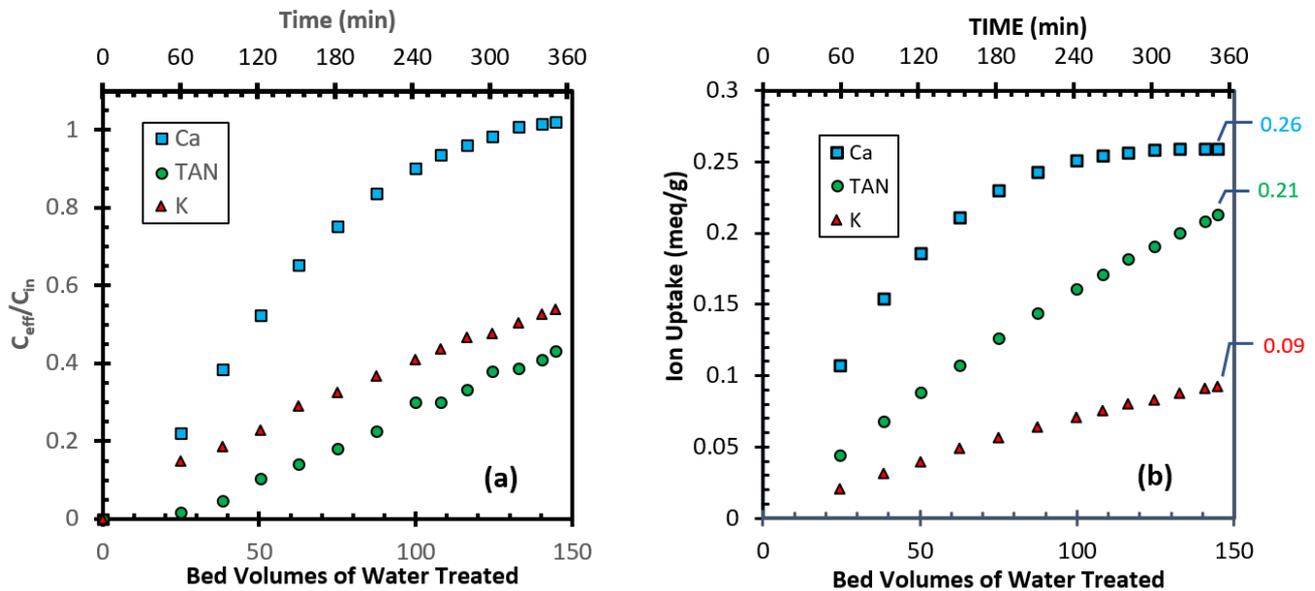


Figure 2. Third 6 h loading cycle with chlorine regeneration (CS3): (a) breakthrough; (b) ion uptake versus bed volumes of water treated.

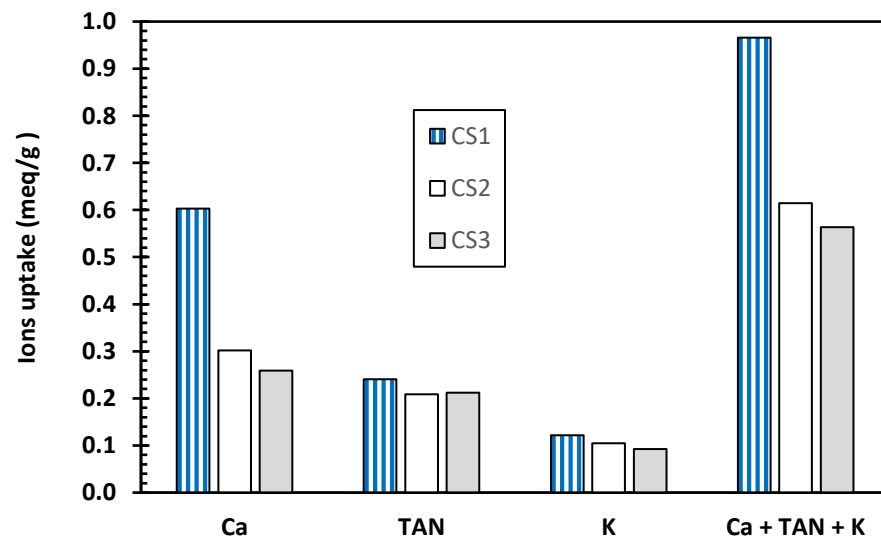


Figure 3. Ion uptakes at the of the CS loading phases.

Figure 4 compares the ion uptakes of the 23 h and 6 h loading cycles that were associated with the NaOCl regeneration. Surprisingly the 6 h loading phase resulted in a higher Ca uptake than the 23 h loading phase. This could be explained by the greater impact of ion competition during the 23 h loading cycle, as evident in the very slow Ca uptake that increased after 80 BVs of water treated in Figure 1b. The TAN, K and total ion uptakes for the 6 h loading phase were smaller (28, 13 and 11%) than those for the 23 h loading phases but not nearly proportional to 3.8 folds difference in the loading cycle durations. Thus, if one uses a two column IE system with one IE column treating EIMWW and the second IE column being regenerated or waiting to go online, then over a one-day period, for the 23 h loading phases there are 1.04 cycles per day whereas for the 6 h loading phases there are 4 cycles per day. These would achieve a removal rate of 0.31 meq TAN/g/day

(i.e., $1.04 \text{ cycle/d} \times 0.30 \text{ meq TAN/g}$) vs. $0.84 \text{ meq TAN/g/day}$ (i.e., $4 \times 0.21 \text{ meq TAN/g}$). Accordingly, over the 24 h period the short loading phases the SIR-600 would remove 2.7 times more TAN.

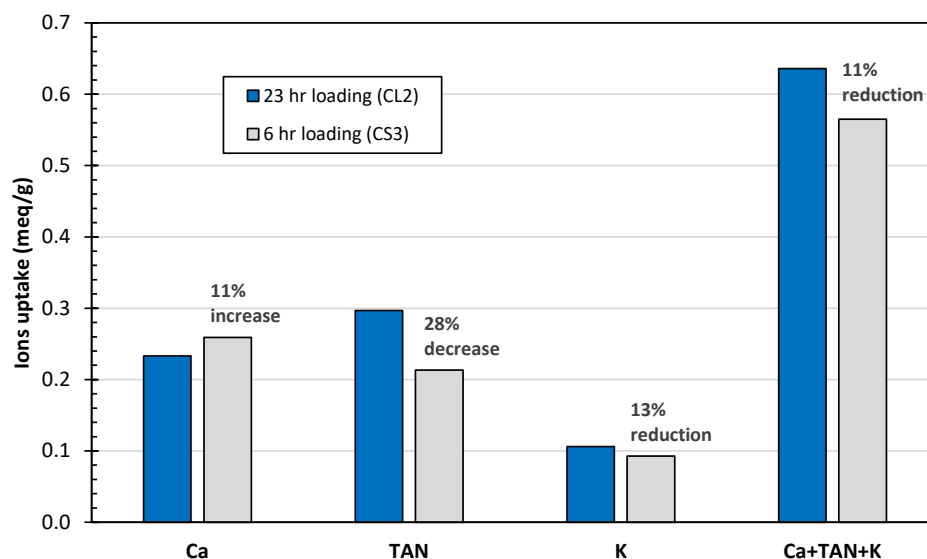
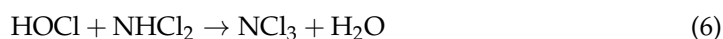


Figure 4. Cumulative ion uptakes at the end of the 23 h and 6 h loading cycles with NaOCl regeneration.

3.3. Chlorine Reactions within the Hypochlorite Regeneration of the Column

The ammonia-chlorine reactions are complex and involve multiple steps and multiple species that are greatly impacted by pH and the $\text{Cl}_2:\text{N}$ ratio [29]. With increasing chlorine addition the following three sequential classical ammonia–chlorine oxidation reactions are as follows [29].



The summation of the monochloramine (NH_2Cl), dichloramine (NHCl_2) and trichloramine (NCl_3), which is referred to as the total chloramines and are the main components of the combined chlorine. With further chlorine additions, NHCl_2 and NCl_3 react to form nitrogen gas. As the raw water does not contain organic compounds and chlorinated organic compounds cannot be formed, the measured combined chlorine consists of these chloramines. It should be noted that the preponderance of the various chloramine species is pH and $\text{Cl}_2:\text{N}$ is ratio-dependent [29]. To investigate the mechanisms of the chlorine regeneration process, the pH, the free chlorine, and total chlorine concentrations were measured in the regeneration effluent samples taken at different times during the regeneration phase.

The data from the CS3 regeneration phase was chosen for presentation (Figure 5) as it was the last cycle and thus more representative of long-term performance. Figure 5 shows the pH values, combined and free chlorine concentrations vs. bed volumes in the regeneration using a 1000 mg/L free Cl_2 solution. The major features of Figure 5 are as follows. First, for the initial 16 BVs of regenerant, the free chlorine concentrations were much lower (below 20 mg Cl_2/L) than the regenerant feed concentration (1000 mg/L) and then increased until they reached approximately 840 mg Cl_2/L at the end of the regeneration process. Thus, it appears that up to 16 BVs of regenerant, all the free chlorine was being consumed. At the end of this regeneration phase, some of the SIR-600 was still being regenerated as still 16% of the free chlorine was being consumed. Given that the effluent-free chlorine profile is similar to a breakthrough curve, it seems the pattern is due to diffusional limitations.

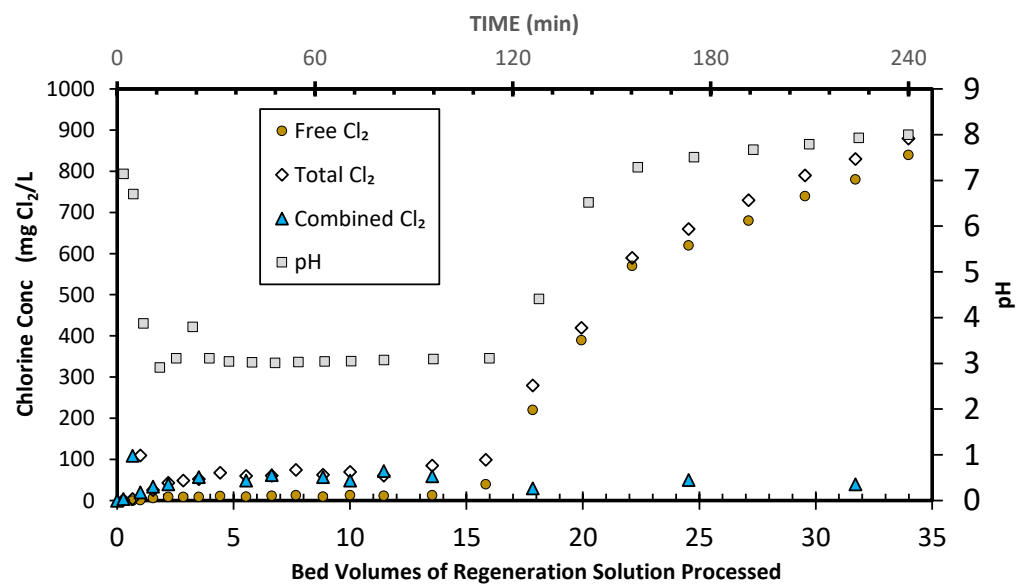


Figure 5. Effluent regenerant water quality during the 4 h-CS3 regeneration: pH, combined chlorine, total chlorine and free chlorine.

Second, the total chlorine follows a very similar pattern to the free chlorine, indicating very low combined chlorine concentrations. Third, the combined chlorine concentration (i.e., the difference between the total and free chlorine concentration) has a small spike at the beginning of the regeneration phase and then stays relatively constant at approximately 40–70 mg /L as Cl₂. It should be noted that influent regenerant also contained a combined chlorine concentration of approximately 40 mg/L as Cl₂. Thus, very little combined chlorine seems to be generated after the initial peak and after 16 BVs of regenerant are processed, the main component of the total chlorine in the effluent is free chlorine. Fourth, the pH of the feed regenerant was ~9.0. Initially, the effluent pH dropped to approximately 3 as the regenerant gradually replaced the distilled water present within the column's voids. After that, the pH remained at approximately 3 till about 16 BVs of regenerant, and then it increased eventually reaching approximately a pH of 8. The pH, free chlorine, and total chlorine follow the same trend: relatively low at the start and gradually increased during the middle of the regeneration phase. As the hypochlorite solution gradually entered the SIR-600 bed, it is hypothesized that the abundant ammonium sorbed on the IE material was rapidly oxidized into nitrogen gas (as suggested by Equation (3)) or possibly other species (e.g., NO₃⁻) with limited “nuisance residual” (NH₂Cl, NCl₃) generated [25]. H⁺ ion generated as a by-product of this reaction, lowered the pH of the effluent.

The following assumptions were made to study the stoichiometric equation. First, the mmoles of ammonia oxidized were estimated by assuming it to be equal to the TAN uptake in the previous loading phase minus the eluted TAN in the following regeneration phase. Using this estimate the amount of the oxidized ammonium was approximately 19 mmol. Secondly, given the free chlorine profile during the regeneration, one could assume it to be complete when the free chlorine concentration in the effluent starts to increase sharply at 16 BV of regenerant. However, it is recognized that the number of regenerant BVs required for the full regeneration should be even higher because it is impossible to determine what the correct value should be. Numerical integration of the free chlorine consumed data up to 16 BV of regenerant yields 25.6 mmoles of free chlorine were consumed. Thus, the estimated molar free chlorine to ammonium ratio would be 1.35 (i.e., 25.6/19). Thus, molar free chlorine to ammonia ratio of 1.5 in Equations (1) and (3) seem reasonable. A second aspect of the stoichiometry that can be investigated is the H⁺ generation based on the changes in pH. Given the influent regenerant pH was equal to ~9, the influent H⁺ concentration is 10⁻⁹ mol/L. Then, using the effluent data, one can calculate the cumulative amount of H⁺ generated as a function of the volume of regenerant processed, which in turn

can be used to calculate the moles H^+ generated per mole of free chlorine consumed. The value of this ratio varied with bed volumes of regenerant processed but its maximum value was 0.057. However, for the CL1 regeneration the pH dropped to approximately 2.35 (data not shown) and the maximum OCl^- / H^+ molar ratio was 0.24, which is still smaller than the 0.666 value predicted by Equation (3). The higher actual pH than the theoretical pH (based on Equation (3)) was possibly due to the reaction between monochloramine and acid, the reaction of hypochlorite ion and the acid, or even possibly reactions between the IE material and the acid.

3.4. Cycles for the 23 h Loading Phases with 5% NaCl Regeneration

The ion breakthroughs of the SL1 cycle were very similar to that of CL1 (Figure S1), indicating that media performed consistently. The ion breakthrough curves of two SL cycles were essentially the same, thus, the 3 h-long 5% NaCl regeneration was effective in restoring the IE capacity of the zeolite. The breakthrough curves for the second cycle (SL2), in terms of the normalized effluent concentration (i.e., C_{eff}/C_{inf}), are presented in Figure 6a, which shows the following. First, the column becomes saturated for Ca first, that is, the effluent concentration reaches the same levels as those in the influent (i.e., $C_{eff}/C_{in} = 1$), at around 400 bed volumes of water treated and plateaus thereafter. Second, the column becomes saturated for TAN at approximately 500 BVs of water treated. Third, the media is not quite saturated with respect to K at the end of the loading run ($C_{eff}/C_{in} = 0.81$ at 586 BVs) and the uptakes are still increasing. Fourth, the order of the breakthroughs (i.e., $Ca \rightarrow TAN \rightarrow K$) is somewhat different from the loading after chlorine regeneration (i.e., $Ca \rightarrow K \rightarrow TAN$). Possible reasons for the deviation were discussed in Section 3.1.

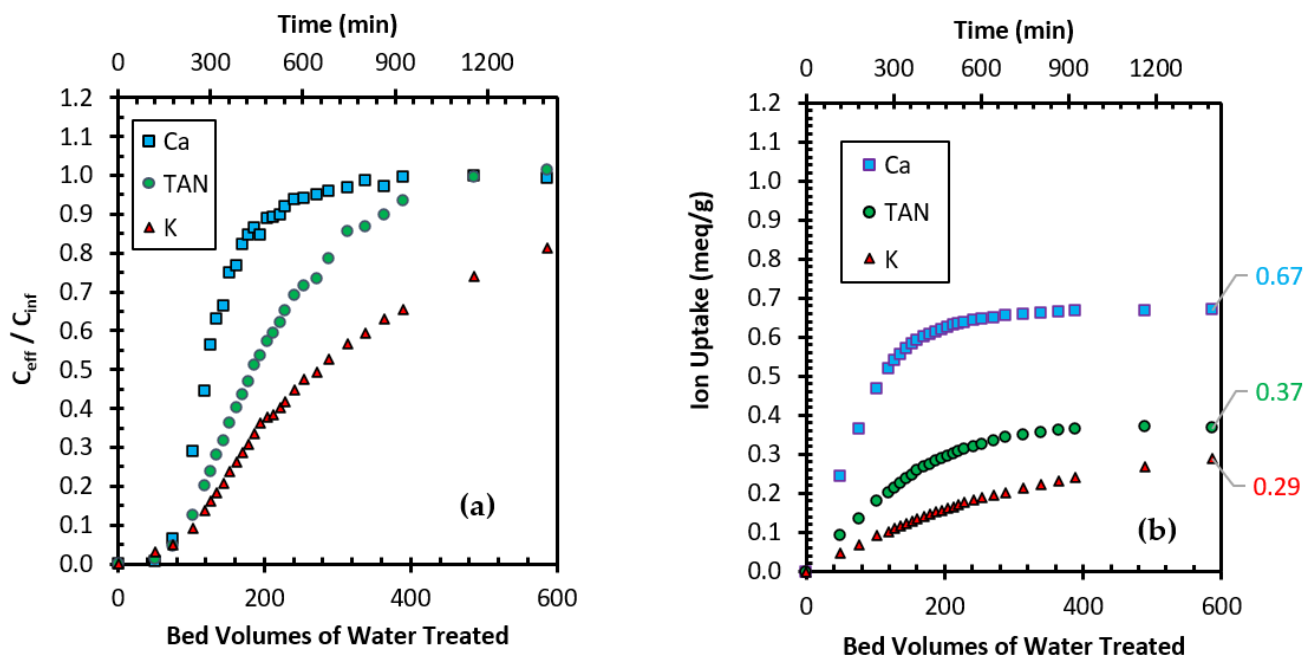


Figure 6. Column's SL2 loading cycle: (a) Ion breakthrough; (b) Ion uptake versus bed volumes of water treated.

The cumulative ion uptakes are presented in Figure 6b. As expected from the very similar breakthrough curve, the ion uptakes achieved in both cycles were very similar as well. The order of the ion uptakes (meq/g) in one loading phase was $Ca > TAN > K$. This order is the same as that of the ion concentrations in the loading solution. Thus, as expected, the ion concentrations (in meq/L) in the feed solution impact the ion uptake in the column loading process when 5% NaCl was applied.

It should be noted that the Ca, TAN and K loadings achieved at the end of the column run (i.e., 0.67, 0.37 and 0.29 meq/g) were 14% lower, 20% higher and 21% higher than

those obtained by Zhang [25] for batch tests using the same water and media. This can be explained by the fact that the equilibrium liquid phase concentrations during the batch tests are lower than those in the EIMWW, while the loadings in the column tend towards to equilibrate with the feed (i.e., the EIMWW). While there are many column studies in the literature, it is difficult to equitably compare the TAN loadings because of the differences between the studies. For studies using clinoptilolite treating solutions with approximately 20 mg/L TAN and using a 2 mg/L breakthrough concentration, the range of TAN uptakes ranges from 0.076 to 0.5 meqTAN/g [18–21,30,31]. For the current run using the same criteria, the TAN uptake is 0.16 meq TAN/g, so the results are comparable particularly given that the current study uses a higher flowrate, smaller particle size media and the pH of the regeneration is not as high.

Figure 6b can also be used to assess the impact of the column kinetics on the ratio of the cumulative uptake of the key ions during the loading phase of the second SL cycle. The TAN:Ca ion uptake ratio increased from 0.4 at 51 BVs to 0.55 at 586 BVs, which means Ca became somewhat less preferable to be absorbed over TAN in IE column during the loading phase. On the other hand, the TAN:K uptake ratio decreased gradually from 51 BVs to 586 BVs (2.0:1 to 1.3:1). The fact that the TAN:K uptake ratio is greater than 1 is consistent with the results using NaOCl regeneration. Furthermore, the column run duration and the breakthrough concentration selected are critical to column performance in terms of the $q_{\text{TAN}}/q_{\text{K}}$ ratios achieved. The $q_{\text{TAN}}/q_{\text{K}} > 1$ result is consistent with the findings of Chartrand et al. [2].

3.5. Cycles for the 6 h Loading Phases with 5% NaCl Regeneration

The three SS cycles (6 h loading + 1 h NaCl regeneration) were conducted to assess the performance of the SIR-600 column with shorter loading and regeneration times. The breakthroughs of the succeeding cycles occurred progressively earlier as the system was adjusting to the new cycle times; however, the difference in the TAN breakthroughs of the second and third SS cycle is relatively small so the system appears to have stabilized. As the third SS cycle should be the most representative of the long-term performance, the subsequent analysis is based on this cycle (SS3). For the 6 h loading cycle, the ion breakthroughs (not shown) followed the same order as that of the 23 h loading phase. Figure 7 shows that, as expected, the ion uptakes were continuously increasing, and they approach but did not reach a plateau level due to the shorter loading phases. The order of the ion uptakes was the same as with the longer loading phases ($q_{\text{Ca}} > q_{\text{TAN}} > q_{\text{K}}$). The SS3 ion uptakes were relatively close to those attained during SS2 after 6 h of operation ($q_{\text{Ca}} = 0.52$ vs. 0.54 meq/g; $q_{\text{TAN}} = 0.21$ vs. 0.22 meq/g; and $q_{\text{K}} = 0.12$ vs. 0.12 meq/g). The differences are attributed to the ongoing re-equilibration of the system and/or a somewhat insufficient regeneration time.

Compared with the ion uptake ratio change in the SL cycles, the ion uptake ratios (TAN:Ca and TAN:K) did not change significantly during the 6-h loading phase of the third SS cycle. This can be explained by the fact that the IE material did not reach or nearly reach the saturation state for any of the three types of ions during the SS loading phases, and the uptake of K was lower leading to less competition for exchange sites. As the column becomes more saturated, the K exerts more competition on the other ions. It should also be noted that there are different ways of quantifying selectivity. In the above experiments, the zeolite column achieved larger uptakes for TAN than K, which suggest SIR-600 has a greater TAN preference in this EIMWW. The greater TAN to K uptake ratio for the shorter loading phases indicates that the dynamics of the column system impact the preference of TAN over K. The $q_{\text{TAN}}/q_{\text{K}}$ ratio greater than one is consistent with the results of Chartrand et al. [2] for their shorter column run (50 BVs, final TAN $C_{\text{eff}}/C_{\text{inf}} = 0.14$). As expected, the Ca, TAN, K and total ion (i.e., Ca + TAN + K) uptakes at the end of SL3 loading cycle were lower than those for the 23 h cycle (22, 43, 60 and 36% lower, respectively). Interestingly, the TAN fraction of the uptake decreased by a much smaller percentage (15%). The ratio of Ca:TAN:K uptake (meq/g) in the SS3 loading phase is 4.5:1.8:1, which is close to the

Ca:TAN:K concentration (in meq/L) ratio in the loading solution (5.2:1.9:1). Comparing the result of loadings in SL cycles, the ion uptake ratios in SS loadings were presumably more related to the ion concentration ratio in the loading solution.

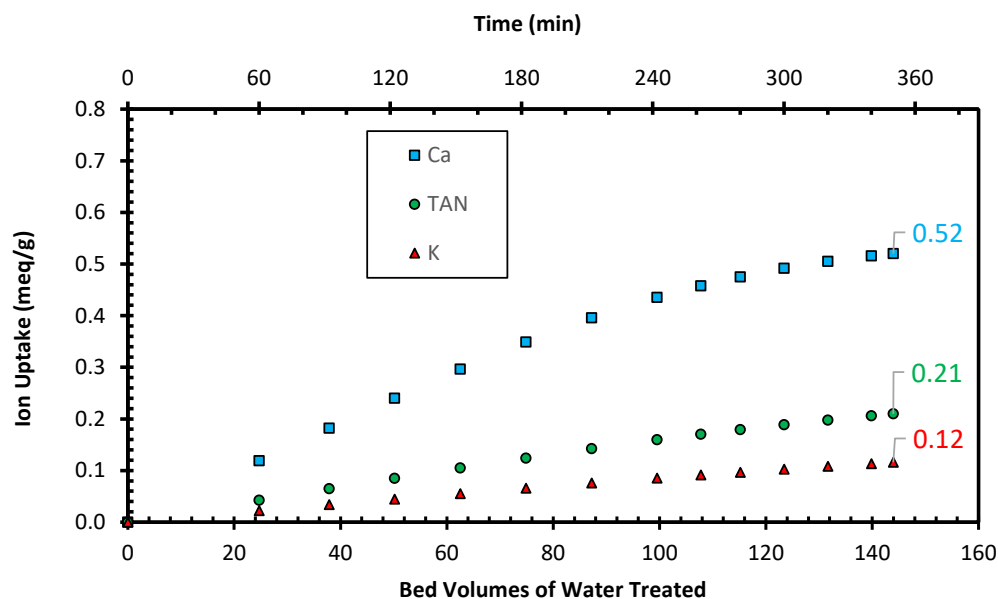


Figure 7. Ion uptake during the loading phase of the SS3 cycle versus bed volumes of water treated.

Based on the salt regeneration cycles and a two-column system, the daily TAN removal rate yields a higher value for the 6 h loading phases than for the 23 h loading phase, that is 0.84 meq TAN/g/day (i.e., 4 cycles/d \times 0.21 meq TAN/g) vs. 0.38 meq TAN/g/day (i.e., 1.04 cycles/d \times 0.366 meq TAN/g). Accordingly, over the 24 h period the short loading phases the SIR-600 would be twice as productive in terms of TAN uptake while using only a somewhat larger volume of NaCl regenerant. In addition, in the shorter cycles, the TAN uptakes are less impacted by competition with K, as the TAN:K ratio increased from 1.3 for the 23 h loading phases to 1.8 for the 6 h loading phases. Thus, the shorter loading phases seem much more efficient and practical.

3.6. Comparison of the Performance with Chlorine Regeneration and Salt Regeneration

The main measures of system performance comparing the performance of the IE systems for ammonium removal from EIMWW are: (a) the TAN uptakes; and (b) regeneration efficiency. A comparison of the loading ion uptakes achieved at the end of the last cycles using 6 h loading phases after salt regeneration (Figure 7) and NaOCl regeneration (Figure 2b) yields Figure 8. First, it clearly shows that NaOCl regeneration decreased the total ion uptake by 33%. The principal reason for the lower total uptake is that: (a) the chlorine primarily targets the TAN regeneration; (b) Na⁺ is present in much smaller concentrations than with salt regeneration (324 mg Na/L vs. 19,658 mg Na/L); and (c) accordingly, only a fraction of the sites occupied by Ca and K get regenerated. Thus, in the subsequent loading cycle, the total ion uptakes decrease. The percent decrease for TAN is much lower than that for the other ions, suggesting that the NaOCl may have altered the selectivity of some sites. Second, the TAN uptake is approximately the same. Comparing the contribution of TAN to the total ion uptake (Figures 2b and 7) it is evident that the TAN fraction of the total ion uptake for chlorine regeneration was 52% higher than for the salt regeneration (i.e., 0.21 meq/g out of 0.56 meq/g versus 0.21 meq/g out of 0.85 meq/g, or 0.38 versus 0.25). Thus, the chlorine regeneration seems to make the system more TAN selective ($q_{\text{TAN}}/q_{\text{K}} = 2.3$ versus 1.75 for 6 h loading cycles). Furthermore, NaOCl regeneration is promising as it achieves essentially the same TAN uptake and avoids the problems of disposing of spent salt regenerant solutions.

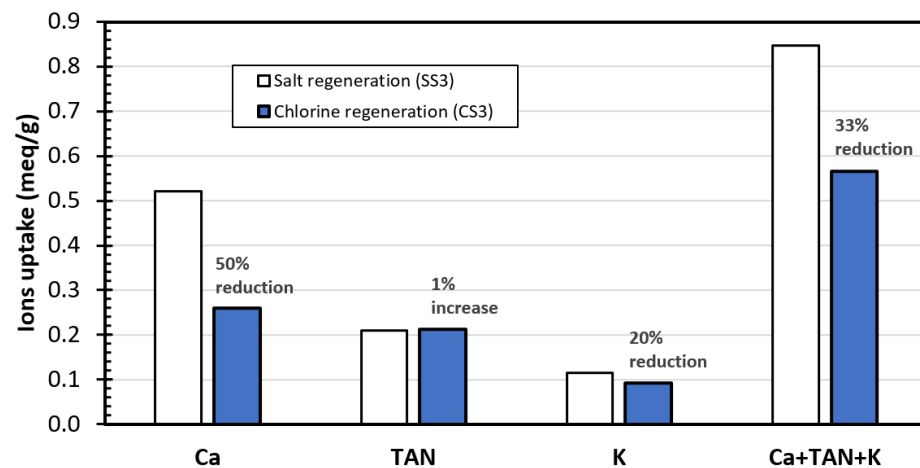


Figure 8. Cumulative ion uptakes at the end of the 6 h loading cycles with NaCl and NaOCl regeneration.

Additional important considerations in the operation of zeolite column systems are the effectiveness and time required to complete the regeneration cycle. During the chlorine regeneration, most of the ammonium reacted with chlorine and was lost from the system as nitrogen gas. As the nitrogen gas was not quantified, it was impossible to conduct a mass balance to assess the TAN released from the IE media and to determine the regeneration efficiency directly by comparing the mass of TAN uptaken and the mass of TAN eluted. Given that after 240 min the effluent-free chlorine concentration and pH have not reached their feed levels (Figure 5), suggests the regeneration is not quite complete. However, the TAN uptake was essentially the same for cycles CS2 and CS3 (Figure 3) the 4 h NaOCl regeneration cycle appeared to be fully effective. Given that 240 min is a much longer regeneration time than predicted by the mass of TAN loaded on the column bed and stoichiometric chlorine requirement to oxidize this ammonia (i.e., ~130 min) suggests there may be other side reactions, non-ideal flow patterns and/or mass transfer limitations.

Ideally, the regeneration phase should be much shorter than the loading phase as there is a need for rinse cycles and it is desirable to have some idle time. The SS series of tests used 6 h loading phases and 1 h regeneration phases, but based on the 80–90% ion recoveries, thus a somewhat longer generation period should be considered. Regardless of this, there is significant idle time. For the CS series, the regeneration was 4 h long so it leaves two hours for the rinsing and idling, which is significantly less but may be sufficient. Based on the effluent regenerant's free chlorine concentrations (Figure 5), it seems that at least 180 min is required for fairly effective regeneration. Initially, much higher chlorine solution flowrates were tried but this led to an excessive quantity of bubbles which impeded the flow, thus it had to be decreased. An alternative would be to use even higher chlorine concentrations, but at 1000 mg/L free chlorine they are already very high and higher concentrations may also lead to the excessive generation of bubbles and/or may lead to the deterioration of the materials within the system. Possibly using a higher flowrate of a lower concentration chlorine regeneration solution may accelerate the chlorine regeneration. Regardless, more research is required into the impact of the key chlorine regeneration operational variables.

Note that although effluent TAN concentration exceeds the common 2 mg/L ($C_{\text{eff}}/C_{\text{inf}} = 0.095$) regulatory standard, this is a proof of concept study. In practice, one would normally use a number of different strategies to reduce the TAN discharge concentrations. These include using shorter loading runs, using larger columns and/or using a lower flowrate. One could add an effluent collection tank with a mixer to collect from the entire loading cycle and blend it to attain a lower average effluent TAN concentration, or one could have several columns in series or several columns in parallel.

It is acknowledged that using 1000 mg/L NaOCl solutions requires the transportation of concentrated NaOCl solution (~12% v/v) to the site and a number of safety precautions. These include a separate chlorine storage and solution preparation area, a containment

system for the concentrated solution storage tank, and a dilution system including a tank, piping and pumps that are not impacted by these chlorine levels. In addition, the materials in the IE column system must also tolerate pHs less than 3 and chlorine concentrations of at least 1000 mg Cl₂/L.

4. Conclusions

The SIR-600 performance in TAN removal from an EMIWW and the effectiveness of different regenerants were tested using multi-cycle bench-scale continuous column loading-regeneration experiments. This represents the first report to study chlorine regeneration of a zeolite column used for the removal of ammonium from a multi-ion solution. The major findings are as follows:

- After operating the column for several operational cycles using 6 h loading phases, chlorine regeneration yielded the same TAN uptakes as NaCl regeneration without producing a regenerant that requires further treatment prior to disposal.
- In the column cycles, the NaOCl regeneration increased SIR-600's TAN preference over K and Ca in the synthetic EIMWW compared to that of NaCl regenerated SIR-600 ($q_{\text{TAN}}/q_{\text{K}} = 2.3$ versus 1.75 for 6 h loading cycles).
- The NaOCl regeneration required longer cycles than the NaCl regeneration.
- It was found that the simultaneous sharp increases in pH, total chlorine and free chlorine concentrations in the effluent regenerant were positively related during the regeneration process, with limited combined chlorine generation (≤ 100 mg/L). This suggests that the oxidation of ammonium into nitrogen gas is the major mechanism behind chlorine regeneration of TAN loaded zeolite.
- Comparing the total cation (Ca, TAN plus K) uptakes after NaOCl regeneration with the TAN uptake achieved by salt regeneration suggests that the Na in the NaOCl regeneration solution played a role in the regeneration.
- Due to the higher TAN mass removal per day, the short duration loading cycles were preferred over the long duration loading cycles.

The above study focuses on the application for a synthetic EIMWW; similar studies should be performed with solutions containing higher TAN concentrations and different TAN:K ratios. More research on the impact of the chlorine concentration, regenerant flowrate and regeneration phase duration is required.

Supplementary Materials: The following supporting information can be downloaded at: <https://www.mdpi.com/article/10.3390/w14193094/s1>, Figure S1. TAN breakthrough for the first 23 h loading cycles of the NaCl and NaOCl regeneration runs (SL1 and CL1).

Author Contributions: The co-authors responsible for the following aspects of this study and manuscript are as follows: conceptualization, R.M.N., M.S. and J.D.; methodology, T.Z., R.M.N., M.S. and J.D.; data analysis, T.Z. and R.M.N.; investigation/experimentation, T.Z.; resources, R.M.N.; writing of original draft, T.Z. and R.M.N.; writing of subsequent drafts, R.M.N.; writing—review and editing, R.M.N. and M.S.; supervision, R.M.N. and M.S.; project administration, R.M.N. and M.S.; funding acquisition, R.M.N., M.S. and J.D. All authors have read and agreed to the published version of the manuscript.

Funding: This research was made possible the support of the VIP Program of the Ontario Centre for Innovation (grant #33021), the Discovery Grant Program of the Natural Sciences and Engineering Research Council of Canada (grant# RGPIN/06571-2018), and our industrial partners Dowclear Environmental Inc. and Milestone Environmental Inc.

Data Availability Statement: The data for this manuscript is available from the lead author's thesis, reference [25].

Conflicts of Interest: This study was partially funded by Dowclear Environmental Inc., whose representative was involved in the choice of the project, the design of the experiments, and the interpretation of the results.

References

1. Forsyth, B.; Cameron, A.; Miller, S. Explosives and Water Quality. In *Proceedings of Sudbury '95: Mining and the Environment, Volume II, Ground and Surface Water*; Hynes, T.P., Blanchette, M.C., Eds.; CANMET: Ottawa, ON, Canada, 1995; pp. 795–803.
2. Chartrand, Z.G.; Narbaitz, R.M.; Sartaj, M.; Downey, J. Ammonia-Ca-K competitive ion-exchange on zeolites in mining wastewater treatment: Batch regeneration and column performance. *J. Sustain. Min.* **2020**, *19*, 59–71. [[CrossRef](#)]
3. Pommen, L.W. *The Effect on Water Quality of Explosives Use in Surface Mining*; Volume 1: Nitrogen Sources, Water Quality, and Prediction and Management of Impacts; Technical Report 4; Ministry of Environment, Water Management Branch: Victoria, BC, Canada, 1983.
4. Randall, D.J.; Tsui, T.K.N. Ammonia toxicity in fish. *Mar. Pollut. Bull.* **2002**, *45*, 17–23. [[CrossRef](#)]
5. Canadian Council of Ministers of the Environment. Canadian Council of Ministers of the Environment. Canadian water quality guidelines for the protection of aquatic life: Ammonia. In *Canadian Environmental Quality Guidelines, 1999*; Canadian Council of Ministers of the Environment: Winnipeg, MB, Canada, 2010.
6. Kleinhenz, L.S.; Trenfield, M.A.; Mooney, T.J.; Humphrey, C.L.; van Dam, R.A.; Nugegoda, D.; Harford, A.J. Acute ammonia toxicity to the larvae (glochidia) of the tropical Australian freshwater mussel *Velesunio* spp. Using a modified toxicity test protocol. *Environ. Toxicol. Chem.* **2018**, *37*, 2175–2187. [[CrossRef](#)] [[PubMed](#)]
7. Environment Canada. Guideline for the Release of Ammonia Dissolved in Water Found in Wastewater Effluents. *Canada Gazette, Part I*, 4 December 2004.
8. ETCC (Environment Technology Center of Canada); Environment Canada. *Biological Test Method: Reference Method for Determining Acute Lethality of Effluents to Rainbow Trout*, 2nd ed.; Environment Canada: Ottawa, ON, Canada, 2000.
9. Hedström, A. Ion exchange of ammonium in zeolites: A literature review. *J. Environ. Eng.* **2001**, *127*, 673–681. [[CrossRef](#)]
10. Huang, J.; Rathnayake Kankanamge, N.; Chow, C.; Welsh, D.T.; Li, T.; Teasdale, P.R. Removing ammonium from water and wastewater using cost-effective adsorbents: A review. *J. Environ. Sci.* **2018**, *2018*, 174–197. [[CrossRef](#)] [[PubMed](#)]
11. Ames, L.L. The cation sieve properties of clinoptilolite. *Am. Mineral.* **1960**, *45*, 689–700.
12. Sarioglu, M. Removal of ammonium from municipal wastewater using natural Turkish (Dogantepe) zeolite. *Sep. Purif. Technol.* **2005**, *41*, 1–11. [[CrossRef](#)]
13. Leyva-Ramos, R.; Aguilar-Armenta, G.; Gonzalez-Gutierrez, L.V.; Guerrero-Coronado, R.M.; Mendoza-Barron, J. Ammonia exchange on clinoptilolite from mineral deposits located in Mexico. *J. Chem. Technol. Biotechnol.* **2004**, *79*, 651–657. [[CrossRef](#)]
14. Guo, X.; Zeng, L.; Li, X.; Park, H.-S. Ammonium and potassium removal for anaerobically digested wastewater using natural clinoptilolite followed by membrane pretreatment. *J. Hazard. Mater.* **2008**, *151*, 125–133. [[CrossRef](#)] [[PubMed](#)]
15. Schoemann, J.J. Evaluation of a South African clinoptilolite for ammonia nitrogen removal from an underground mine water. *Water SA* **1986**, *12*, 73–82.
16. Dryden, H.T.; Weatherley, L.R. Aquaculture water treatment by ion exchange: Continuous ammonium ion removal with clinoptilolite. *Aquac. Eng.* **1989**, *8*, 109–126. [[CrossRef](#)]
17. Rahmani, A.; Mahvi, A.; Mesdaghinia, A.; Nasser, S. Investigation of ammonia removal from polluted waters by Clinoptilolite zeolite. *Int. J. Environ. Sci. Technol. (Tehran)* **2004**, *1*, 125–133. [[CrossRef](#)]
18. Chartrand, Z. The Selective Ion-Exchange Removal of Ammonia from Mining Wastewater. Master's Thesis, Department of Civil Engineering, University of Ottawa, Ottawa, ON, Canada, 2018. [[CrossRef](#)]
19. ResinTech Inc. Resintech SIR-600. 2020. Available online: https://www.resintech.com/rks_images/shopcart/pdf_specs_90253.pdf (accessed on 15 May 2021).
20. Koon, J.H.; Kaufman, W.J. Ammonia removal from municipal wastewater by ion exchange. *J. Water Pollut. Control Fed.* **1975**, *47*, 448–465.
21. Semmens, M.J.; Booth, A.C.; Tauxe, G.W. Clinoptilolite column ammonia removal model. *J. Environ. Engr. Div. (ASCE)* **1978**, *104*, 231–244. [[CrossRef](#)]
22. Deng, Q.; Elbeshbishy, E.; Lee, H.-S. Simultaneous regeneration of exhausted zeolite and nitrogen recovery using air stripping method at alkaline pH. *Water Qual. J. Can.* **2016**, *51*, 321–330. [[CrossRef](#)]
23. Huang, H.; Yang, L.; Xue, Q.; Liu, J.; Hou, L.; Ding, L. Removal of ammonium from swine wastewater by zeolite combined with chlorination for regeneration. *J. Environ. Manag.* **2015**, *160*, 333–341. [[CrossRef](#)] [[PubMed](#)]
24. Zhang, W.; Zhou, Z.; An, Y.; Du, S.; Ruan, D.; Zhao, C.; Ren, N.; Tian, X. Optimization for zeolite regeneration and nitrogen removal performance of a hypochlorite-chloride regenerant. *Chemosphere* **2017**, *178*, 565–572. [[CrossRef](#)] [[PubMed](#)]
25. Zhang, T. Ammonia Removal from Mining Wastewater by Ion-Exchange Regenerated by Chlorine Solutions. Master's Thesis, Department of Civil Engineering, University of Ottawa, Ottawa, ON, Canada, 2022. [[CrossRef](#)]
26. ASTM D6913/D6913M-17; Standard Test Methods for Particle-Size Distribution (Gradation) of Soils Using Sieve Analysis. ASTM International: West Conshohocken, PA, USA, 2017. Available online: www.astm.org (accessed on 10 May 2021).
27. APHA. *Standard Methods for the Examination of Water and Wastewater*, 18th ed.; American Public Health Association: Washington, DC, USA, 1992. Available online: [https://www.scirp.org/\(S\(351jmbntvnsjt1aadkposzje\)\)/reference/ReferencesPapers.aspx?ReferenceID=1818549](https://www.scirp.org/(S(351jmbntvnsjt1aadkposzje))/reference/ReferencesPapers.aspx?ReferenceID=1818549) (accessed on 30 August 2022).
28. APHA. *Standard Methods for the Examination of Water and Wastewater*, 23rd ed.; American Public Health Association: Washington, DC, USA, 2017. Available online: <https://scirp.org/reference/referencpapers.aspx?referenceid=2329795> (accessed on 30 August 2022).

29. Black and Veatch Corp. *White's Handbook of Chlorination and Alternative Disinfectants*, 5th ed.; John Wiley & Sons, Inc.: Hoboken, NJ, USA, 2010.
30. Svetich, R. Long-term use of clinoptilolite in the treatment of sewage at Tahoe-Truckee Sanitation Agency, Truckee, California. In *Proceedings of the 4th International Conference on the Occurrence, Properties, and Utilization of Natural Zeolites*, Boise, ID, USA, 20–28 June 1993.
31. Vociante, M.; De Folly D'Auris, A.; Finocchi, A.; Tagliabue, M.; Bellettato, M.; Ferruci, A.; Reverberi, A.P.; Ferro, S. Adsorption of ammonium on clinoptilolite in presence of competing cations: Investigation on groundwater remediation. *J. Clean. Prod.* **2018**, *198*, 480–487. [[CrossRef](#)]